



HAL
open science

Driving Power Supply for Ultrasound Piezoelectric Transducers

Modar Jomaa, François Costa, Dejan Vasic, Pierre-Etienne Lévy, Marwan Ali

► **To cite this version:**

Modar Jomaa, François Costa, Dejan Vasic, Pierre-Etienne Lévy, Marwan Ali. Driving Power Supply for Ultrasound Piezoelectric Transducers. 2023 IEEE International Conference on Electrical Systems for Aircraft, Railway, Ship Propulsion and Road Vehicles & International Transportation Electrification Conference (ESARS-ITEC), Mar 2023, Venice, Italy. 10.1109/ESARS-ITEC57127.2023.10114888 . hal-04461710

HAL Id: hal-04461710

<https://hal.science/hal-04461710>

Submitted on 16 Feb 2024

HAL is a multi-disciplinary open access archive for the deposit and dissemination of scientific research documents, whether they are published or not. The documents may come from teaching and research institutions in France or abroad, or from public or private research centers.

L'archive ouverte pluridisciplinaire **HAL**, est destinée au dépôt et à la diffusion de documents scientifiques de niveau recherche, publiés ou non, émanant des établissements d'enseignement et de recherche français ou étrangers, des laboratoires publics ou privés.

Driving Power Supply for Ultrasound Piezoelectric Transducer

Modar Jomaa
SATIE ENS Paris-Saclay
Université de Paris-Saclay
Gif-sur-Yvette, France
modar.jomaa@ens-paris-saclay.fr

François Costa
SATIE ENS Paris-Saclay
Université de Paris Est Creteil
Gif-sur-Yvette, France
francois.costa@ens-paris-saclay.fr

Dejan Vasic
SATIE ENS Paris-Saclay
Université de Cergy-Pontoise
Gif-sur-Yvette, France
dejan.vasic@ens-paris-saclay.fr

Pierre-Etienne Lévy
SATIE ENS Paris-Saclay
Université de Paris-Saclay
Gif-sur-Yvette, France
pierre-etienne.levy@ens-paris-saclay.fr

Marwan Ali
SAFRAN SA
Magny les Hameaux, France
marwan.ali@safrangroup.com

Abstract— Piezoelectric actuators are widely used in several applications and are becoming increasingly attractive in aircraft and industrial contexts, mainly when efficient and economical energy conversion is required. One of these applications is the Avionic Piezoelectric Deicing System. Since piezoelectric actuators exhibit a distinct capacitive behavior in almost all frequencies, designing their driving power supply presents a major challenge, especially for deicing applications requiring high operational frequency. This article discusses and analyzes the comparison between three converter topologies for piezoelectric applications. The comparison is based on specific criteria, such as varying the operating frequency with the load variation, soft-switching operation, and reactive energy compensation. Based on this comparison, the chosen converter was developed and realized in the laboratory.

Keywords—Piezoelectric actuator, resonant inverter, PWM inverter, soft-switching converter, reactive energy compensation.

I. INTRODUCTION

Environmental constraints and their impact on public opinion have led the aircraft industry to accelerate the energy transition in aeronautics through the "More Electric Aircraft". We are therefore witnessing a gradual increase in the role of electrical energy in onboard applications. This electrification trend aims to replace all non-propulsive systems (hydraulic and pneumatic) with electromechanical ones in order to optimize aircraft performance, decrease operating and maintenance costs, increase dispatch reliability, and reduce gas emissions.

Among the systems underscored by this transition is the deicing system. A variety of deicing methods that defer by the energy used are employed today to prevent ice formation. These include: turbine engine bleed air, pneumatic deice boot system, Chemical Fluid, and Electrically Heated Systems [1, p. 2]. However, these methods are classified as very energy consuming and are only suitable for some aircraft categories.

The proposed study aims to identify a converter topology adapted to piezoelectric actuators for deicing applications. After presenting the specifications of the converter, a survey by simulation of several topologies is conducted to identify their advantages for our application. A demonstrator of the selected solution is then developed to validate our choice.

II. SPECIFICATIONS

A. Application: Piezoelectric Deicing System

The operating principle of the piezoelectric deicing system is to generate microscopic mechanical ultrasonic vibration based on the principle of the inverse piezoelectric effect. These electromechanical vibrations produce a stress field at the interface leading edge/ice great enough to delaminate the ice. This new method can be applied using piezoelectric stacks or Langevin Transducers, which are to be bonded on the interior of the leading edge's surface via rigid glue (for the stacks) or mechanical fixation with a bolt (for the transducers) as illustrated in Fig. 1.

Several studies have been conducted on this deicing system, with different types of piezoelectric actuators and on various frequency ranges. A study on the deicing efficiency of these two architectures concluded that transducers are more advantageous in terms of power consumption, mechanical failure (fracture of the ceramics), and structural fatigue and that deicing is more favorable beyond 20 kHz [2].

In order to properly drive an ultrasound transducer and improve its performance, it is essential to know its electrical characteristics. The most common equivalent circuit that characterizes a piezoelectric actuator around its resonance frequency is the Van Dyke model. In this model, we identify the static capacitance C_s paralleled with a motional branch (L_m , C_m , R_m). Each piezoelectric transducer has several resonance frequencies in which its impedance has a lower magnitude as compared to non-resonance frequencies. To attain higher efficiency and deliver more power to the ultrasound system, the transducer will be excited at its main resonance frequency at 123 kHz (Fig. 2).

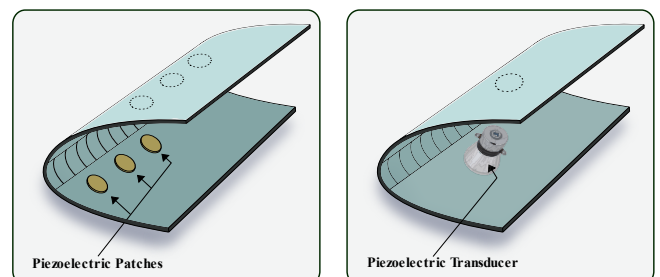


Fig. 1. Configuration of a piezoelectric deicing system with piezoelectric patches and transducers

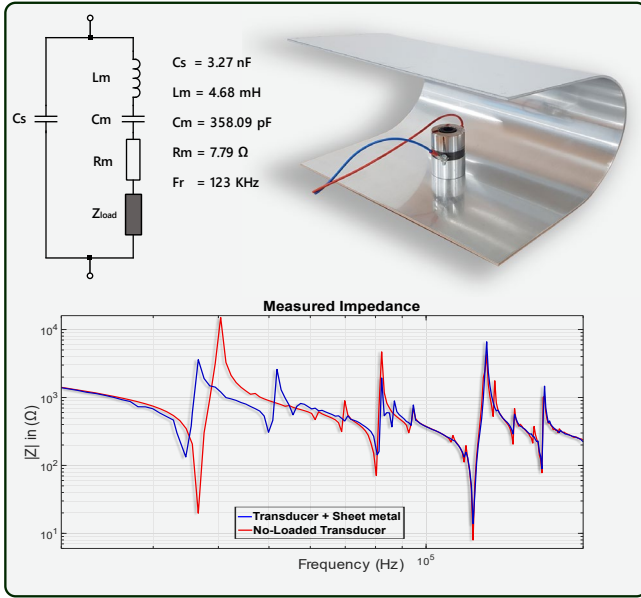


Fig. 2. Characterization of the piezoelectric transducer by the Van Dyke model around the resonance frequency at 123 kHz.

B. Electrical specifications

The deicing system and its power supply must comply with the aviation regulations and standards (DO 160), as well as the installation constraints of the equipment (safety, space requirements), while allowing its proper operation.

The power supply should deliver a sinusoidal voltage to the transducer in order to excite the desired mode. Otherwise, undesired harmonics (low-quality signal) can deteriorate the transducer's performance and increase power consumption in the system.

Finally, Given the space constraints that do not allow to place the converter to be as close as possible to the load (transducer), the latter will be fed through 2 meters length cables.

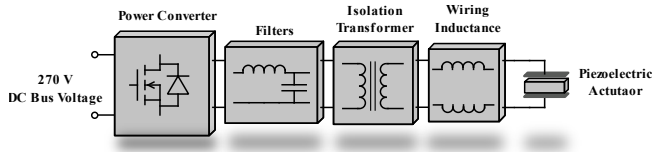


Fig. 3. Synoptic board of the complete system.

III. INVESTIGATED TOPOLOGIES

Since the electrical behavior depends on the mechanical load and the temperature, it's essential to consider some aspects when designing the power supply. One is the driving frequency which must correspond to the mechanical resonance frequency of the actuator attached to the leading edge. In fact, at this resonance, the power transfer is better, and the reactive energy consumption is reduced (less loss). Another important aspect is the quality of the excitation signal, which has an important role in the piezoelectric transducer's performance and lifetime [3].

In this context, several techniques are proposed in the literature [4],[5],[6]. Linear power amplifiers (A, B, AB, ...) are used to feed piezoelectric loads because they can generate signals with low harmonic distortion rates. However, they

have low efficiency and are often bulky and heavy. Therefore, switched-mode power supplies are more and more used and dominate the market because of their good efficiency and high power density.

In this regard, various literatures have focused on driving piezoelectric actuators using voltage source inverters. Resonant inverters (LC or LLC) and PWM inverters (LC or LLC) are the most commonly used. Other topologies have been used, such as the three-level NPC inverter and the current inverter [7]. The main disadvantages of resonant inverters are the volume and weight of the magnetic elements of the resonant filter and a very limited variation of the operating frequency. To overcome these drawbacks, PWM-controlled inverters (LC or LLC) have been proposed [8]. The disadvantages of PWM control are always related to the switching frequency, which generates high switching losses and EMC constraints.

A. Current Source Inverter (CSI)

Conventional converters usually use LC filters to improve the quality of the excitation signal. However, the inductive and capacitive characteristics added by the filter can deteriorate the performance of the transducer by shifting its resonance frequency. Given that a piezoelectric actuator has a capacitive behavior on almost all its frequency ranges, a current source inverter can be a good choice to drive the transducer and have a favorable effect on its performance.

Simulation conditions: the current source inverter is fed through a buck converter at 270 V to control its output current. The schematic of the complete system is shown in Fig. 4, where Z_{load} represents the impedance of the mechanical load set to 0Ω for our simulations. The CSI is operated using a unipolar full-wave control at the mechanical resonance frequency of the transducer.

Given that the CSI imposes a square-wave current and the motional branch absorbs a sinusoidal current I_m , the static

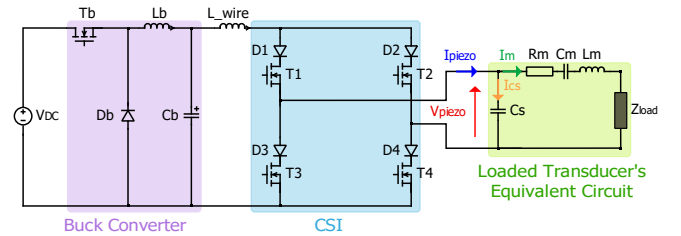


Fig. 4. Circuit topology of the complete system (Buck + CSI + Loaded Transducer)

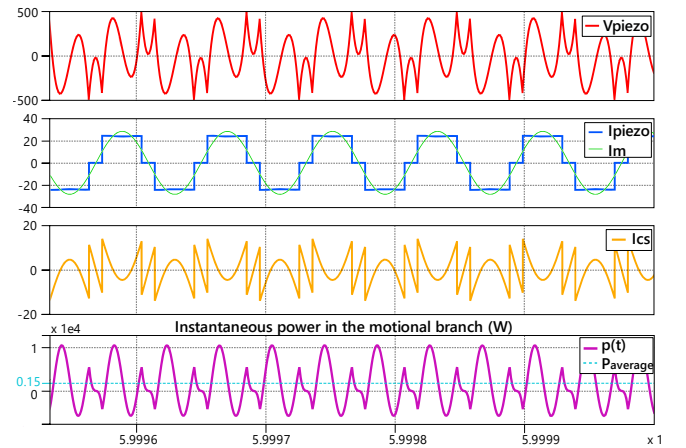


Fig. 5. CSI's output waveforms.

capacitance C_s absorbs the difference I_{C_s} defining the waveform of V_{piezo} (Fig. 5). Actually, to have a sinusoidal output voltage, an inductance should be added in parallel with the capacitance C_s and drive the CSI at their own resonance frequency. However, this added inductance establishes with C_s a highly selective bandpass filter that would limit the operating frequency range in addition to a very strong attenuation of the fundamental current.

This topology will not be retained regarding the specifications that impose a sinusoidal output voltage. Moreover, with the addition of the wiring inductance and the isolation transformer, the load seen by the CSI will be inductive, causing important voltage spikes on the CSI transistors, which can decrease the quality and efficiency of the system.

B. Energy Recovery "Resonant" Converter

Driving piezoelectric actuators using standard converters usually leads to a significant power loss at any switching cycle due to the capacitive nature of the load. Therefore, conventional converters integrate an inductor which is, in most cases, heavy and bulky, making the system unsuitable for some applications, especially aeronautics. This problem has led to numerous studies aiming to optimize the power factor [9], [10]. The system's volume can also be impacted by oversizing power converters due to switching losses. It is then necessary to introduce zero-voltage switching techniques that usually use large inductors [11].

In this regard, a new topology with an auxiliary shunt circuit has attracted our attention [12]. The circuit includes a switching arm and a small auxiliary inductance. This inductance is not in the path of the major power flow. Therefore, it is not designed according to the actuator's resonance frequency.

In order to adapt this structure to our application case, the output voltage must be bipolar. For this, the modification in Fig. 6 has been proposed.

This structure allows us to achieve the zero-voltage-switching (ZVS) condition on the four switching cells. It also allows us to recover the reactive energy from the static capacitor and thus increase the converter's efficiency. However, if the transducer is driven with a square-wave voltage, several mechanical resonance modes are excited, leading to possible cracks in the piezoelectric ceramics. To solve this problem, a low-pass filter should be implemented. However, by adding the filtering inductance, the ZVS switching condition is no more ensured. This condition depends on the resonance between $(L1+L2)$ and C_s . Therefore, an adjustment of the dead time should be considered with any inductance added (wiring inductance,

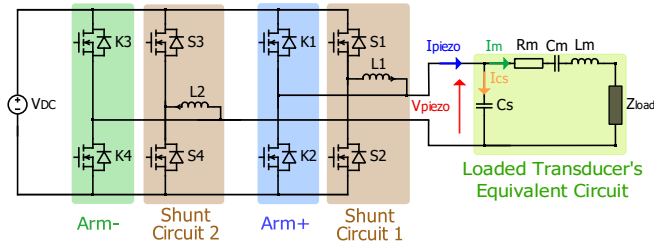


Fig. 6. Circuit topology of the energy recovery "resonant" converter.

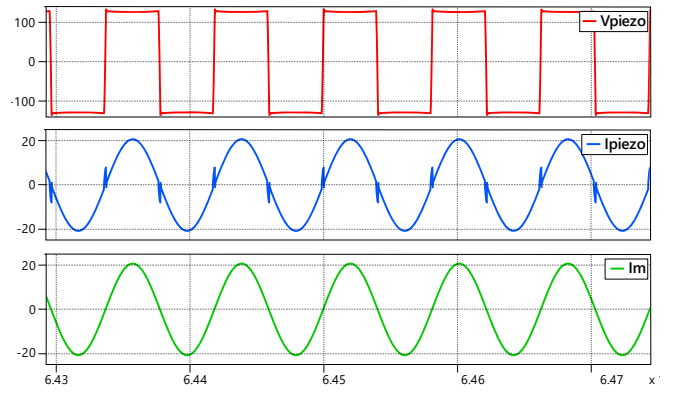


Fig. 7. "Resonant" converter's output waveforms.

the leakage inductance of the isolation transformer ...), implying a less-than-optimal power transmission to the load.

This structure is interesting for driving a piezoelectric load directly at a fixed frequency. However, with all the constraints of our specifications, it would be complicated to adopt this topology.

C. Auxiliary Resonant Commutated Pole Inverter (ARCPI)

Several soft-switching inverter topologies have been proposed in the literature [13],[14],[15]. This type of inverter aims to achieve high-frequency operation with reduced switching losses and electromagnetic interference (EMI). An interesting example of soft-switching inverters of the "Resonant Pole Inverter (RPI)" family is the Auxiliary Resonant Commutated Pole Inverter (ARCPI) [16],[17]. The circuit topology, and its theoretical waveforms, are illustrated in Fig. 8 and Fig. 9, respectively.

The inverter consists of two main arms and an auxiliary circuit connected to a capacitive divider bridge. In order to limit losses as well as the number of components, one arm is switched at Low Frequency (LF) synchronized to the transducer frequency, and the other is switched at High Frequency (HF), on which the auxiliary circuit is connected. The role of this circuit is to charge and discharge the parasitic capacitances C_{oss} to ensure ZVS condition on the HF arm. On the other hand, the control law of the auxiliary circuit implies zero current switching (ZCS) of its transistors. Moreover, since the auxiliary circuit is not in the main power path, the power rating of its switches will be reduced compared to that of the main switches. The control applied is a unipolar PWM which reduces the output voltage harmonics.

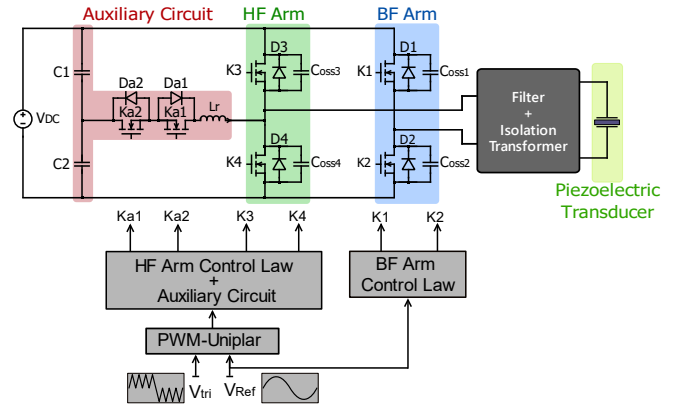


Fig. 8. Circuit topology of the ARCP Inverter.

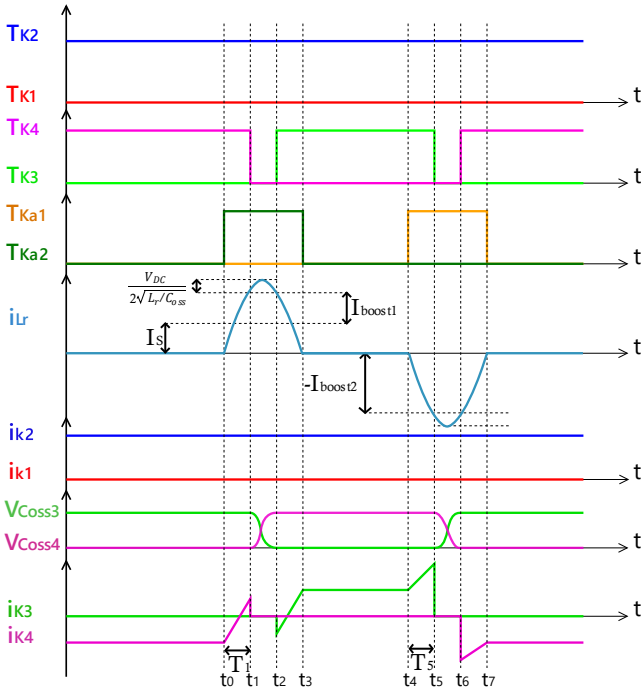


Fig. 9. ARCPI theoretical waveforms.

Resonant inductance sizing:

To achieve ZVS on all main switches of the HF arm, the stored energy in the resonant inductance L_r must be sufficient to charge and discharge the parasitic capacitances of the concerned transistors. Therefore, the following conditions must be respected:

$$\frac{V_{DC}}{2L_r} T_1 \geq I_{s_{max}} \quad \text{et} \quad \frac{V_{DC}}{2L_r} T_5 \geq I_{s_{max}} \quad (1)$$

With $T_1 = t_1 - t_0$ et $T_5 = t_5 - t_4$.

From (1):

$$L_r \leq \frac{V_{DC} \cdot T_1 \cdot V_{s_{max}}}{4P_{s_{max}}} \quad (2)$$

With: $P_{s_{max}} = \frac{1}{2} V_{s_{max}} I_{s_{max}}$

Simulation:

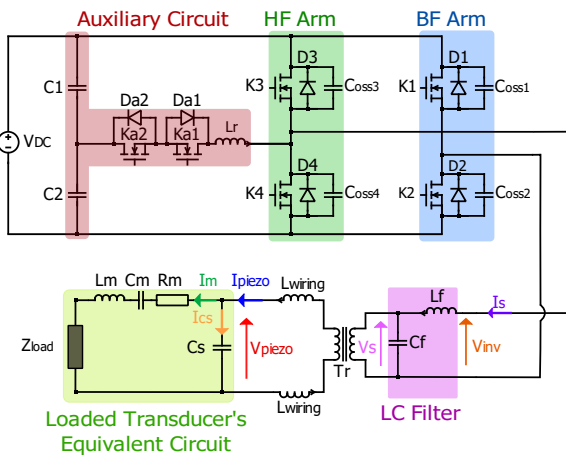


Fig. 10. Circuit topology of the complete system (ARCPI + LC filter + isolation transformer + wiring inductance + loaded transducer).

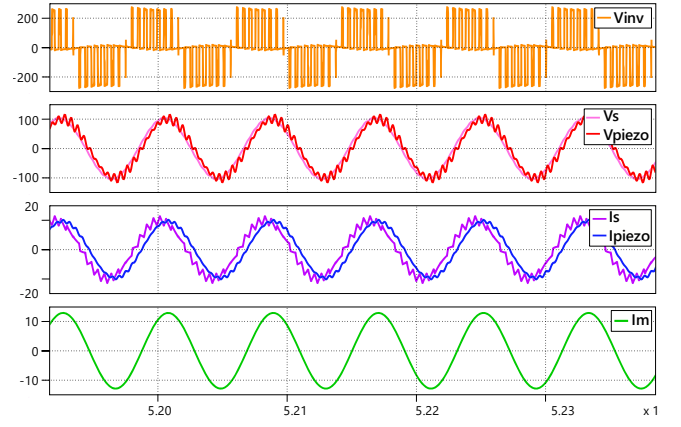


Fig. 11. ARCPI output waveforms.

The inverter output filter was sized to have a current ripple of less than 20%. I_s and a cutoff frequency $f_{LC} = f_{sw}/10$, knowing that $f_{sw} = 2 \text{ MHz}$. This implies $L_f = 8.5 \mu\text{H}$ and $C_f = 76 \text{ nF}$.

The simulation is performed taking into account the wiring inductance ($2 \cdot L_{wiring} = 2 \mu\text{H}$). Fig. 11 shows sinusoidal waveforms with a total harmonic distortion (THD) of 13% for the voltage V_{piezo} across the transducer, and 5% for the output current I_s . The relatively high THD on V_{piezo} is due to the resonance between the wiring inductance and the transducer's static capacitance C_s . This resonance deteriorates the operation of the filter leading to low attenuation and even amplification of some harmonics around this resonance. The choice of the output filter is not definitive. The use of an LLC filter might be considered later.

Finally, the advantages of the ARCPI over the topologies mentioned above (see Table I) make it ideal for our application.

TABLE I. TOPOLOGIES COMPARATIVE TABLE

Topology	CSI	"Resonant" Converter	ARCPI
Frequency sweeping	☹️	☹️	😊
Sensitivity to load variation	☹️	😊	😊
Soft-switching	😊	😊	😊
Reactive energy compensation	☹️	😊	😊
Control law	😊	😊	😊

Experimental Results

The experimental setup of the ARCP Inverter was built, as shown in Fig. 12, in order to validate the simulation results with the experimental measurement. The control of the inverter has been implemented in an FPGA. A first implementation was done on a Texas Instrument DSP but proved limited in modulation frequency.

All measuring signals are monitored using an oscilloscope. Initial measurements were made on a stable RL ($30 \Omega + 96 \mu\text{H}$) load to validate the proper operation of the converter.



Fig. 12. Experimental setup of the ARCP Inverter.

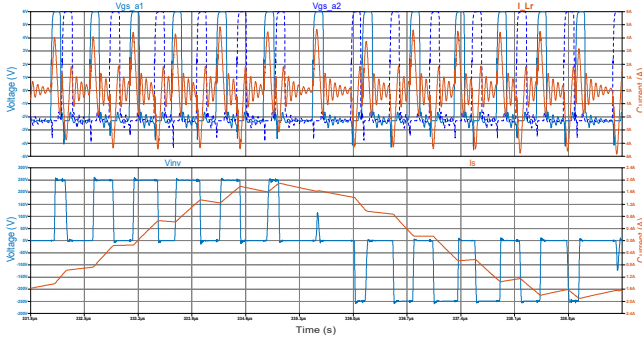


Fig. 13. LTspice simulation waveforms: V_{gs_a1} , V_{gs_a2} , I_{Lr} , V_{inv} , I_s .

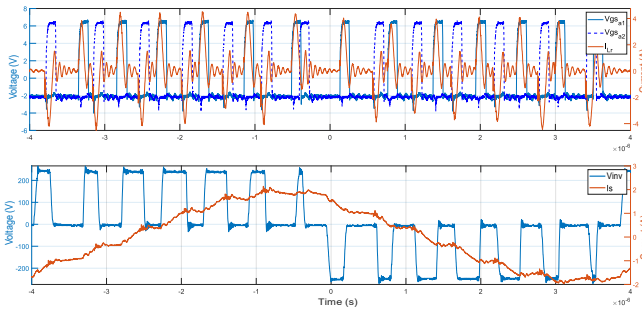


Fig. 14. Experimental waveforms: V_{gs_a1} , V_{gs_a2} , I_{Lr} , V_{inv} , I_s .

The BF arm is switched at the low frequency (125 kHz) synchronized to the output voltage while the HF arm is switched at high frequency at 2MHz, under 250 Vdc bus voltage.

The simulation results match very well with the experimental measurements, which is reassuring (Fig. 13 et Fig. 14). By visualizing the current I_{Lr} in the resonant inductance, we can verify the correct operation of the auxiliary circuit where we see the charging, discharging and resonance phases between L_r and $2C_{oss}$.

CONCLUSION

In the context of the "More Electric Aircraft" project which this contribution is a part of, a study of different converter topologies for driving piezoelectric deicing system has been carried out. The ARCPI topology was privileged due to many advantages outlined above. An experimental setup was built, which ensured the validation of the simulation results. The next step is to test the inverter on a representative load under icing conditions in order to validate the piezoelectric deicing concept.

REFERENCES

- [1] « Aviation Maintenance Technician Handbook - Airframe Volume 2 », p. 564.
- [2] M. Budinger, V. Pommier-Budinger, G. Napias, et A. Costa da Silva, « Ultrasonic Ice Protection Systems: Analytical and Numerical Models for Architecture Tradeoff », *J. Aircr.*, vol. 53, no 3, p. 680-690, mai 2016, doi: 10.2514/1.C033625.
- [3] Rongyuan Li, N. Frohlike, et J. Bocker, « LLC-PWM inverter for driving high-power piezoelectric actuators », in 2008 13th International Power Electronics and Motion Control Conference,

- Poznan, Poland, sept. 2008, p. 159-164. doi: 10.1109/EPEPEMC.2008.4635261.
- [4] K. Agbossou, J.-L. Dion, S. Carignan, M. Abdelkrim, et A. Cheriti, « Class D amplifier for a power piezoelectric load », *IEEE Trans. Ultrason. Ferroelectr. Freq. Control*, vol. 47, no 4, p. 1036-1041, juill. 2000, doi: 10.1109/58.852087.
- [5] H. L. Cheng, C. A. Cheng, C. C. Fang, et H. C. Yen, « Single-switch high power factor inverter for driving piezoelectric ceramic transducer », in 2009 International Conference on Power Electronics and Drive Systems (PEDS), Taipei, nov. 2009, p. 1571-1576. doi: 10.1109/PEDS.2009.5385732.
- [6] Sai Chun Tang et G. T. Clement, « A harmonic cancellation technique for an ultrasound transducer excited by a switched-mode power converter », in 2008 IEEE Ultrasonics Symposium, Beijing, China, nov. 2008, p. 2076-2079. doi: 10.1109/ULTSYM.2008.0513.
- [7] S. M. R. Sadriyeh, M. R. Zolghadri, et J. Mahdavi, « Application of a current source inverter for a linear piezoelectric step motor drive », in 4th IEEE International Conference on Power Electronics and Drive Systems. IEEE PEDS 2001 - Indonesia. Proceedings (Cat. No.01TH8594), Denpasar, Indonesia, 2001, vol. 2, p. 892-897. doi: 10.1109/PEDS.2001.975438.
- [8] C. Kauczor et N. Frohlike, « Inverter topologies for ultrasonic piezoelectric transducers with high mechanical Q-factor », in 2004 IEEE 35th Annual Power Electronics Specialists Conference (IEEE Cat. No.04CH37551), Aachen, Germany, 2004, p. 2736-2741. doi: 10.1109/PESC.2004.1355265.
- [9] B. Duchame, L. Garbuio, M. Lallart, D. Guyomar, G. Sebald, et J.-Y. Gauthier, « Nonlinear Technique for Energy Exchange Optimization in Piezoelectric Actuators », *IEEE Trans. Power Electron.*, vol. 28, no 8, p. 3941-3948, août 2013, doi: 10.1109/TPEL.2012.2227813.
- [10] Y.-P. Liu et D. Vasic, « Small power step-up converter for driving flapping wings of the micro robotic insects », in 2012 IEEE Energy Conversion Congress and Exposition (ECCE), Raleigh, NC, USA, sept. 2012, p. 41-46. doi: 10.1109/ECCE.2012.6342414.
- [11] W.-C. Su et C.-L. Chen, « ZVS for PT Backlight Inverter Utilizing High-Order Current Harmonic », *IEEE Trans. Power Electron.*, vol. 23, no 1, p. 4-10, janv. 2008, doi: 10.1109/TPEL.2007.911831.
- [12] D. Vasic et F. Costa, « Energy recovery power supply for piezoelectric actuator », in IECON 2014 - 40th Annual Conference of the IEEE Industrial Electronics Society, Dallas, TX, USA, oct. 2014, p. 1440-1445. doi: 10.1109/IECON.2014.7048691.
- [13] D. M. Divan, « The resonant DC link converter-a new concept in static power conversion », *IEEE Trans. Ind. Appl.*, vol. 25, no 2, p. 317-325, avr. 1989, doi: 10.1109/28.25548.
- [14] D. C. Katsis, J.-Y. Choi, D. Boroyevich, et F. C. Lee, « Drive Cycle Evaluation of A Soft-Switched Electric Vehicle Inverter », p. 6.
- [15] J.-Y. Lim, J. Soh, et R.-Y. Kim, « An Improved Single-Phase Zero-Voltage Transition Soft-Switching Inverter with a Subtractive Coupled Inductor Auxiliary Circuit », in 2016 IEEE Vehicle Power and Propulsion Conference (VPPC), Hangzhou, China, oct. 2016, p. 1-6. doi: 10.1109/VPPC.2016.7791610.
- [16] R. W. De Doncker et J. P. Lyons, « The auxiliary resonant commutated pole converter », in Conference Record of the 1990 IEEE Industry Applications Society Annual Meeting, Seattle, WA, USA, 1990, p. 1228-1235. doi: 10.1109/IAS.1990.152341.
- [17] M.-C. Jiang, W.-S. Wang, H.-K. Fu, et K. Wu-Chang, « A novel single-phase soft-switching unipolar PWM inverter », in 8th International Conference on Power Electronics - ECCE Asia, Jeju, Korea (South), mai 2011, p. 2874-2879. doi: 10.1109/ICPE.2011.5944785.